

**Ammonium-based and phosphonium-based temperature control-type polyoxometalate ionic liquids**

Journal:	<i>Dalton Transactions</i>
Manuscript ID:	DT-ART-04-2014-001146.R1
Article Type:	Paper
Date Submitted by the Author:	01-Jul-2014
Complete List of Authors:	Li, Yunyan; Zhejiang University, Department of Chemistry Wu, Xuefei; Zhejiang University, Department of Chemistry Wu, Qingyin; Zhejiang University, Department of Chemistry Ding, Hong; Jilin University, State Key Laboratory of Inorganic Synthesis and Preparative Chemistry Yan, Wenfu; Jilin University, State Key Laboratory of Inorganic Synthesis and Preparative Chemistry

Cite this: DOI: 10.1039/c0xx00000x

ARTICLE TYPE

www.rsc.org/xxxxxx

Ammonium-based and phosphonium-based temperature control-type polyoxometalate ionic liquids

Yunyan Li,^a Xuefei Wu,^a Qingyin Wu,^{*a} Hong Ding,^b and Wenfu Yan^b

Received 18th April 2014, Accepted Xth July 2014

DOI: 10.1039/b000000x

Ammonium-based and phosphonium-based polyoxometalate ionic liquids (POM-ILs) have been synthesized and characterized. The results of small-angle XRD patterns indicate that phosphonium-based POM-IL possesses layered type structure. They are both temperature control-type POM-ILs and can exhibit a phase transformation below 100 °C. Phosphonium-based POM-IL exhibits higher thermal stability and conductivity than its ammonium analogue.

Introduction

Polyoxometalates (POMs) are early transition metal oxygen clusters that can be synthesized in many different sizes and with variety of heterometals. In recent years, attentions have been focused on them due to not only their special intrinsic structure but also their potential application in the fields of catalysis, photochemistry, electrochemistry, medicine, biology, magnetism, fuel cells.¹⁻⁶

Ionic liquids, which are normally composed of relatively large organic cations and inorganic anions, have attracted great interest for their excellent properties, such as negligible volatile pressure, low toxicity, high thermal stability, high conductivity, as well as the ability to dissolve a wide range of organic and inorganic compounds.⁷⁻⁹

Many kinds of functional ionic liquids have been synthesized, most of them are the ones with functional groups appended to the cationic moieties.¹⁰⁻¹² Recently, a family of ionic liquids in which the anions incorporate active constituents have been explored. In this context, POMs would seem to offer considerable promise as the basis for functional ionic liquids due to their diverse properties. Polyoxometalate-based ionic liquids (POM-ILs) have received much attention in recent years because they are studied as promising electrolytes in various fields such as fuel cells and supercapacitors.¹³⁻¹⁷ Their design and synthesis can also broaden the application of heteropoly acids (HPAs) greatly, which suffer from high sensitivity to atmospheric moisture, diffusional problems, relatively weak thermal stability and continuous leakage during cell operation. So far, tetralkylammonium cation, tetraalkylphosphonium cation, imidazolium and pyridinium derivative all have been employed for the synthesis of these

POM-ILs. However, a great deal of attention has been given to ammonium-based POM-ILs, phosphonium-based POM-ILs have received far less attention as electrolytes,^{18,19} although they have found some applications in catalysis.²⁰⁻²² Study of the relationship between ammonium-based and phosphonium-based POM-ILs is scarce. So we chose tributyltetradecylammonium bromide (TBTAB) and tributyltetradecylphosphonium chloride (TBTPC) to synthesize two new POM-ILs. They are not sensitive to atmospheric moisture due to their hydrophobic nature. The phosphonium-based POM-IL shows attractive advantages in terms of thermal stability and conductivity over its ammonium analogue as non-aqueous electrolyte.

Experimental section

Synthesis of POM-ILs

H₆PW₉V₃O₄₀ was synthesized according to the procedure described in our previous report.²³

Tributyltetradecylammonium bromide (TBTAB) was synthesized by modification of the method according to the literatures available.²⁴

H₆PW₉V₃O₄₀ and TBTAB (TBTPC) were taken in 1:6 (1:6) mole ratio to give one mole of [TBTA]₆PW₉V₃O₄₀ ([TBTP]₆PW₉V₃O₄₀). TBTAB (TBTPC) was dropped into the ethanol solution of H₆PW₉V₃O₄₀ under continuous stirring. Upon addition of the entire TBTAB (TBTPC), red product formed, which was stirred at room temperature for 24h. The product was washed with ethanol and dried in vacuum at room temperature to give the final one which exhibits gel-like state. The obtained compounds are highly insoluble in water and ethanol, soluble in ethyl acetate, acetone, dichloromethane and dimethyl sulfoxide.

Instrument and reagent

FTIR spectrum was measured on a Nicolet Nexus 470 FT/IR spectrometer over the wave number range 400-4000 cm⁻¹ using KBr pellets. UV spectrum was obtained on a SHIMADZU U-2550 UV-Vis spectrophotometer. Small-angle XRD pattern was

^a Department of Chemistry, Zhejiang University, Hangzhou 310027, PR China. Fax: +86 571 87951895; Tel: +86 571 88914042;

⁴⁵ E-mail: qyw@zju.edu.cn (Q.Y. Wu)

^b State Key Laboratory of Inorganic Synthesis and Preparative Chemistry, Jilin University, Changchun 130012, PR China.

measured on a D/Max-2550 diffractometer operated at 50 KV and 200 mA in the range of $2\theta = 2-10^\circ$ at a rate of $0.5^\circ \cdot \text{min}^{-1}$. Wide-angle XRD pattern was recorded on a BRUKER D8 ADVANCE X-ray diffractometer using a Cu tube operated at 40 kV and 40 mA in the range of $2\theta = 25-35^\circ$ at a rate of $0.02^\circ \cdot \text{s}^{-1}$. The thermal stability of the sample was studied using thermogravimetry (TG) and differential thermal analysis (DTA) techniques from room temperature to 600°C . Measurement was performed using a Shimadzu thermal analyzer in a Nitrogen stream, with a scanning rate of $10^\circ\text{C} \cdot \text{min}^{-1}$. Conductivity was measured by a DDS-11A conductivity meter fitted with a Shanghai DJS-1 electrode. The conductivity meter was calibrated by the standard KCl solution with a concentration of $0.01 \text{ mol} \cdot \text{L}^{-1}$.

All chemicals were of analytical grade and used without further purification.

Results and discussion

The neat HPA ($\text{H}_6\text{PW}_9\text{V}_3\text{O}_{40}$), its ammonium-based and phosphonium-based POM-ILs are characterized by the IR spectra in Fig. 1. The four characteristic bands of the Keggin structure of $\text{H}_6\text{PW}_9\text{V}_3\text{O}_{40}$ (curve a) appeared at 1070 , 976 , 879 and 795 cm^{-1} , assignable to vibrations of $\text{P}-\text{O}_a$, $\text{M}-\text{O}_d$, $\text{M}-\text{O}_b-\text{M}$ and $\text{M}-\text{O}_c-\text{M}$ ($\text{M} = \text{W}, \text{V}$), respectively.²⁵ In spite of slight changes in wavenumbers and intensities, the four Keggin-structured peaks of $[\text{TBTA}]_6\text{PW}_9\text{V}_3\text{O}_{40}$ (curve b) and $[\text{TBTP}]_6\text{PW}_9\text{V}_3\text{O}_{40}$ (curve c) are also observed distinctly. This result indicates that the two POM-ILs still retain Keggin structure after the protons of HPA are substituted by organic cations. Compared with the parent HPA, clear red shifts for the $\text{M}-\text{O}_d$ band and blue shifts for the $\text{M}-\text{O}_c-\text{M}$ ($\text{M} = \text{W}, \text{V}$) band are presented of these two POM-ILs. The shifts illustrate that an interaction exists between the organic cation and the heteropoly anion. From the geometry of the anion, the anion-cation interactions cause certain charge-density repartition in the compounds.²⁶ Meanwhile, $[\text{TBTA}]_6\text{PW}_9\text{V}_3\text{O}_{40}$ and $[\text{TBTP}]_6\text{PW}_9\text{V}_3\text{O}_{40}$ present the new characteristic bands in the region of $3000-2850 \text{ cm}^{-1}$ and $1500-1380 \text{ cm}^{-1}$ which are attributed to C-H stretching and C-H bending vibrations, respectively. The vibrations of C-N and C-P bonds are weak and may be overlapped with C-C and $\text{P}-\text{O}_a$ vibrational bands in the region of $1250-1000 \text{ cm}^{-1}$.

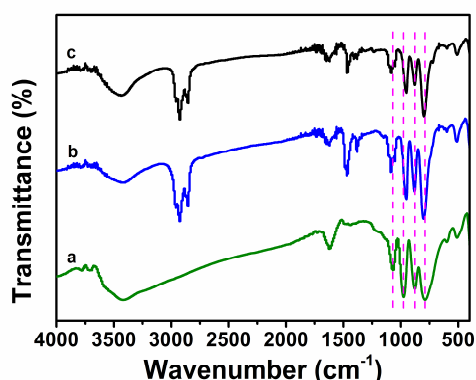


Fig. 1 IR spectra of $\text{H}_6\text{PW}_9\text{V}_3\text{O}_{40}$ (a), $[\text{TBTA}]_6\text{PW}_9\text{V}_3\text{O}_{40}$ (b) and $[\text{TBTP}]_6\text{PW}_9\text{V}_3\text{O}_{40}$ (c).

UV spectra of these two POM-ILs are recorded using dichloromethane as the solvent, shown in Fig. 2. The characteristic bands at 254 nm for $[\text{TBTA}]_6\text{PW}_9\text{V}_3\text{O}_{40}$ and 256 nm for $[\text{TBTP}]_6\text{PW}_9\text{V}_3\text{O}_{40}$ are due to charge-transfer of bridge-oxygen (O_b, O_c) to metal atoms (W, V) in the heteropolyanion cage. When compared with the parent HPA, the characteristic peaks of $[\text{TBTA}]_6\text{PW}_9\text{V}_3\text{O}_{40}$ and $[\text{TBTP}]_6\text{PW}_9\text{V}_3\text{O}_{40}$ show some slight shifts, which is in good agreement with that of the IR spectra [23]. The result also indicates that the size of the cation influences greatly on the anion-cation interactions.²⁷

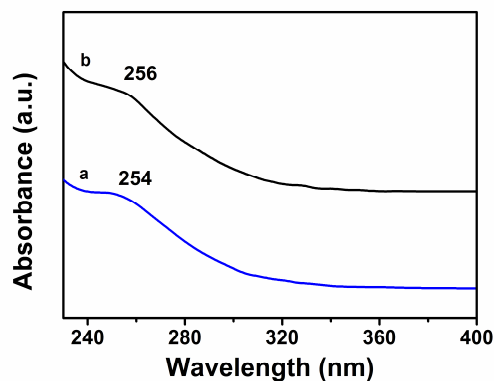


Fig. 2 UV spectra of $[\text{TBTA}]_6\text{PW}_9\text{V}_3\text{O}_{40}$ (a) and $[\text{TBTP}]_6\text{PW}_9\text{V}_3\text{O}_{40}$ (b).

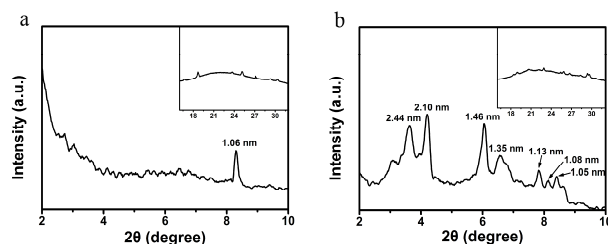


Fig. 3 Small-angle XRD patterns of $[\text{TBTA}]_6\text{PW}_9\text{V}_3\text{O}_{40}$ (a) and $[\text{TBTP}]_6\text{PW}_9\text{V}_3\text{O}_{40}$ (b). Inset: Corresponding wide-angle XRD patterns.

The phase and structure of $[\text{TBTA}]_6\text{PW}_9\text{V}_3\text{O}_{40}$ and $[\text{TBTP}]_6\text{PW}_9\text{V}_3\text{O}_{40}$ are further studied by using powder X-ray diffraction (XRD) in Fig. 3. In the wide-angle region, the XRD patterns of the two POM-ILs both present a very broad peak at the region of $2\theta = 16-32^\circ$, which is consistent with the amorphous nature of the samples.²⁸ However, their parent HPA displays the crystal structure according to the literature.²³ The results mean that in synthesis of $[\text{TBTA}]_6\text{PW}_9\text{V}_3\text{O}_{40}$ and $[\text{TBTP}]_6\text{PW}_9\text{V}_3\text{O}_{40}$, the original structure of $\text{H}_6\text{PW}_9\text{V}_3\text{O}_{40}$ is rearranged by introduction of TBTP and TBTA cations, involving the self-assembly of cations and anions through electrostatic interactions and Van der Waals forces.²⁹ It also demonstrates that the secondary structure of HPA derivatives is influenced greatly by the nature of the cations. In the small-angle region, the two POM-ILs display different Bragg diffraction peaks, which are attributed to their different layered structures. Only one Bragg diffraction peak is shown in the XRD pattern of $[\text{TBTA}]_6\text{PW}_9\text{V}_3\text{O}_{40}$, which is the characteristic peak of Keggin structure at the region of $2\theta = 7-10^\circ$.³⁰ However, in the small-angle region of XRD curve of $[\text{TBTP}]_6\text{PW}_9\text{V}_3\text{O}_{40}$, seven sharp peaks are present, which arises from the regular arrangement of the molecules in layers. The larger five peaks are the characteristic peaks of Keggin structure.

And, the smaller two peaks during 3 to 5° indicate two types of layered structures with spacing values of 2.44 and 2.10 nm exist. In the simulations, the lengths of the alkyl chains are estimated considering the planar zigzag conformations. The thickness of a single layer is calculated as 3.34 nm, considering the lengths of the anion and cation are 1.04 and 2.30 nm, respectively.³¹ This value is larger than the thickness value obtained by the XRD pattern (2.44 and 2.10 nm). So the cations display staggered arrangement around the anions or there is conformational disorder of chains. Schematic illustration of two possible types of layered structures is shown in Fig. 4.

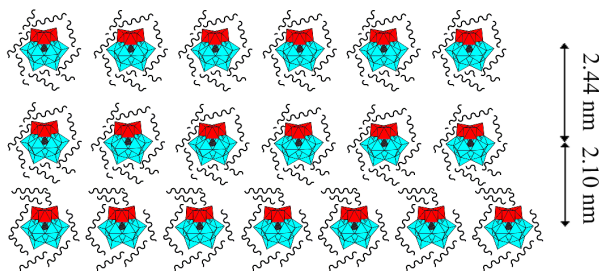


Fig. 4 Schematic illustration of two possible types of layered structures of [TBTP]₆PW₉V₃O₄₀. Color legend of PW₉V₃O₄₀⁶⁻: WO₆ blue octahedra, VO₆ red octahedra, PO₄ black tetrahedra.

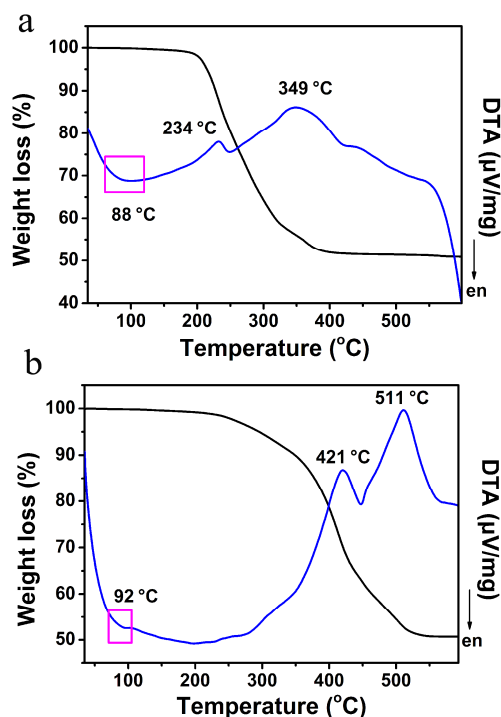


Fig. 5 TG-DTA curves of [TBTA]₆PW₉V₃O₄₀ (a) and [TBTP]₆PW₉V₃O₄₀ (b).

Fig. 5 shows the TG-DTA curves of both POM-ILs in N₂ at a heating rate of 10 K min⁻¹. The TG curves of [TBTA]₆PW₉V₃O₄₀ and [TBTP]₆PW₉V₃O₄₀ both exhibit a one-step weight loss process, which is attributed to the decomposition of the organic and inorganic moieties. The weight loss of 49.09 wt.% (calc. 49.58%) for [TBTA]₆PW₉V₃O₄₀ and 49.31 wt.% (calc. 50.63%) for [TBTP]₆PW₉V₃O₄₀ are due to the release of organic moieties and oxide (P₂O₅). The DTA curves of [TBTA]₆PW₉V₃O₄₀ and

[TBTP]₆PW₉V₃O₄₀ show the endothermic peaks in the heating process, indicating the two POM-ILs display the phase transformation from solid state to liquid state. Photographs of thermo-responsive behavior of the POM-ILs are shown in Fig. 6. The exothermic peaks of DTA curves demonstrate the decomposition of organic moieties and inorganic moieties gradually. The decomposition temperature (*T_d*) is recorded according to the first exothermic peak of the DTA curve.³² The *T_d* of [TBTA]₆PW₉V₃O₄₀ (234 °C) is much lower than that of [TBTP]₆PW₉V₃O₄₀ (421 °C), which indicates that the tetraalkylphosphonium cations contribute to improve the thermal stability of such POM-ILs.³³

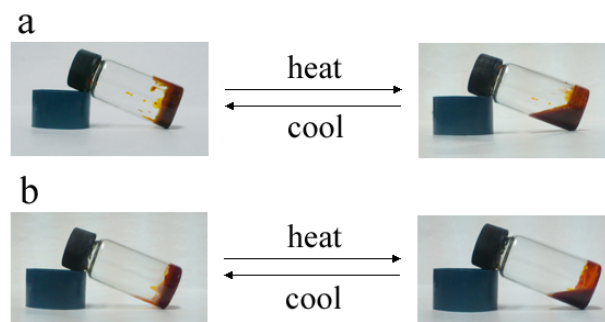


Fig. 6 Photographs of thermo-responsive behavior of [TBTA]₆PW₉V₃O₄₀ (a) and [TBTP]₆PW₉V₃O₄₀ (b).

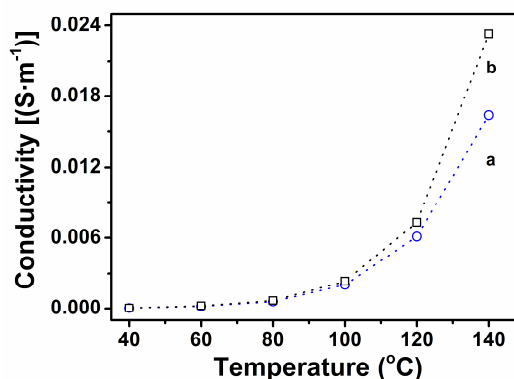


Fig. 7 Conductivity versus temperature plots of [TBTA]₆PW₉V₃O₄₀ (a) and [TBTP]₆PW₉V₃O₄₀ (b).

The conductivity of [TBTA]₆PW₉V₃O₄₀ and [TBTP]₆PW₉V₃O₄₀ in the temperature range from 313.15 to 413.15 K is shown in Fig. 7. Conductivity of these compounds increases with higher temperature as the mobility of conducting species increases with temperature.³⁴ Under the same conditions, [TBTP]₆PW₉V₃O₄₀ has higher conductivity than [TBTA]₆PW₉V₃O₄₀. Part of the reason may be that phosphonium-based POM-IL has weaker Coulombic interaction than its ammonium analogue, as the Coulombic interaction between the cation and the anion of the POM-IL tends to cause a decrease in mobility.³⁵ The increase of conductivity before 100 °C is smaller than the increase of conductivity after 100 °C. So the conductivity of these POM-ILs are dependent on temperature.

In this paper we have reported the syntheses, characterization, conductive performance of two POM-ILs, [TBTA]₆PW₉V₃O₄₀ and [TBTP]₆PW₉V₃O₄₀, which are based on Keggin structure

HPA. XRD patterns indicate that phosphonium-based POM-IL possesses layered type structure due to the self-assembly of cations and anions through electrostatic interactions and Van der Waals forces while ammonium-based POM-IL does not. They are both temperature control-type POM-ILs and can exhibit a phase transformation below 100 °C. Phosphonium-based POM-IL exhibits higher thermal stability and conductivity than its ammonium analogue. The higher conductivity of phosphonium-based POM-IL may be due to its weaker Coulombic interactions. The phosphonium-based POM-IL is expected to be promising non-aqueous electrolyte for electrochemical applications.

Acknowledgements

This work was funded by the National Nature Science Foundation of China (21071124, 21173189), the Zhejiang Provincial Natural Science Foundation of China (LY14B030005) and the Foundation of State Key Laboratory of Inorganic Synthesis and Preparative Chemistry of Jilin University (2013-06).

References

- 1 A. M. Khenkin, I. Efremenko, J. M. L. Martin and R. Neumann, *J. Am. Chem. Soc.*, 2013, **135**, 19304.
- 2 J. Cuan and B. Yan, *Dalton Trans.*, 2013, **42**, 14230.
- 3 J. Suárez-Guevara, V. Ruiz and P. Gomez-Romero, *J. Mater. Chem. A*, 2014, **2**, 1014.
- 4 J. T. Rhule, C. L. Hill and D. A. Judd, *Chem. Rev.*, 1998, **98**, 327.
- 5 J. M. Clemente-Juan, E. Coronado and A. Gaita-Ariño, *Chem. Soc. Rev.*, 2012, **41**, 7464.
- 6 (a) X. Tong, X. F. Wu, Q. Y. Wu, W. M. Zhu, F. H. Cao and W. F. Yan, *Dalton Trans.*, 2012, **41**, 9893; (b) Q. Y. Wu, X. Y. Qian and S. M. Zhou, *Xuzhou Inst. Tech. (Nat. Sci. Ed.)*, 2012, **27**, 1.
- 7 L. Timperman, H. Galiano, D. Lemordant and M. Anouti, *Electrochem. Commun.*, 2011, **13**, 1112.
- 8 X. Q. Sun, H. M. Luo and S. Dai, *Chem. Rev.*, 2012, **112**, 2100.
- 9 I. Skarmoutsos, T. Welton and P. A. Hunt, *Phys. Chem. Chem. Phys.*, 2014, **16**, 3675.
- 10 D. Fang, X. L. Zhou, Z. Ye and Z. L. Liu, *Ind. Eng. Chem. Res.*, 2006, **45**, 7982.
- 11 S. G. Lee, *Chem. Commun.*, 2006, **42**, 1049.
- 12 K. Pöhako-Esko, T. Taaber, K. Saal, R. Löhmus, I. Kink and U. Mäeorg, *Synth. Commun.*, 2013, **43**, 2846.
- 13 A. B. Bourlinos, K. Raman, R. Herrera, Q. Zhang, L. A. Acher and E. P. Giannelis, *J. Am. Chem. Soc.*, 2004, **126**, 15358.
- 14 P. G. Dickert, M. R. Antonio, M. A. Fierstone, K. A. Kubatko, T. Szreder, J. F. Wishart and M. L. Dietz, *Dalton Trans.*, 2007, **36**, 529.
- 15 F. Yan, S. Yu, X. Zhang, L. Qiu, F. Chu, J. You and J. Lu, *Chem. Mater.*, 2009, **21**, 1480.
- 16 X. F. Wu, X. Tong, Q. Y. Wu, H. Ding and W. F. Yan, *J. Mater. Chem. A*, 2014, **2**, 5780.
- 17 T. L. Greaves and C. J. Drummond, *Chem. Rev.*, 2008, **108**, 206.
- 18 L. Timperman, H. Galiano, D. Lemordant and M. Anouti, *Electrochem. Commun.*, 2011, **13**, 1112.
- 19 L. Timperman and M. Anouti, *Ind. Eng. Chem. Res.*, 2012, **51**, 3170.
- 20 M. Picquet, S. Stutzmann, I. Tkatchenko, I. Tommasi, J. Zimmermann and P. Wasserscheid, *Green Chem.*, 2003, **5**, 153.
- 21 B. Mariampillai, J. Alliot, M. Li and M. Lautens, *J. Am. Chem. Soc.*, 2007, **129**, 15372.
- 22 P. Thansandote, D. G. Hulcoop, M. Langer and M. Lautens, *J. Org. Chem.*, 2009, **74**, 1673.
- 23 X. Tong, N. Q. Tian, W. Wu, W. M. Zhu, Q. Y. Wu, F. H. Cao, W. F. Yan and A. B. Yaroslavtsev, *J. Phys. Chem. C*, 2013, **117**, 3258.
- 24 S. A. Buckingham, C. J. Garvey and G. G. Warr, *J. Phys. Chem.*, 1993, **97**, 10236.
- 25 D. Y. Chen, A. Sahasrabudhe, P. Wang, A. Dasgupta, R. X. Yuan and S. Roy, *Dalton Trans.*, 2013, **42**, 10587.
- 26 L. D. Chen, X. S. Wang, X. W. Guo, H. C. Guo, H. Liu and Y. Y. Chen, *Chem. Eng. Sci.*, 2007, **62**, 4469.
- 27 Z. Y. Li, Q. Zhang, H. T. Liu, P. He, X. D. Xu and J. H. Li, *J. Power Sources*, 2006, **158**, 103.
- 28 X. F. Wu, Y. Y. Li, X. Tong and Q. Y. Wu, *Funct. Mater. Lett.*, 2014, **7**, 1450019.
- 29 X. Yan, P. Zhu, J. Fei and J. Li, *Adv. Mater.*, 2010, **22**, 1283.
- 30 X. Tong, N. Q. Tian, W. M. Zhu, Q. Y. Wu, F. H. Cao and W. F. Yan, *J. Alloys Compd.*, 2012, **544**, 37.
- 31 M. H. Godinho, C. Cruz, P. I. C. Teixeira, A. J. Ferreira, C. Costab, P. S. Kulkarni and C. A. M. Afonso, *Liq. Cryst.*, 2008, **35**, 103.
- 32 Q. Y. Wu, X. Q. Cai, W. Q. Feng, W. Q. Pang, *Thermochim. Acta*, 2005, **428**, 15.
- 33 K. Tsunashima, S. Kodama, M. Sugiya and Y. Kunugi, *Electrochim. Acta*, 2010, **56**, 762.
- 34 C. Tiyyapiboonchaiya, J. M. Pringle, J. Z. Sun, N. Byrne, P. C. Howlett, D. R. Macfarlane and M. Forsyth, *Nat. Mater.*, 2004, **3**, 29.
- 35 J. S. Luo, O. Conrad and I. F. J. Vankelecom, *J. Mater. Chem.*, 2012, **22**, 20574.